A Review of Remote Sensing Image Fusion Methods

Hassan Ghassemian

PII: S1566-2535(16)30017-3
DOI: 10.1016/j.inffus.2016.03.003
Reference: INFFUS 775

To appear in: *Information Fusion*

Received date: 13 October 2015
Revised date: 27 January 2016
Accepted date: 14 March 2016

Please cite this article as: Hassan Ghassemian , A Review of Remote Sensing Image Fusion Methods, *Information Fusion* (2016), doi: 10.1016/j.inffus.2016.03.003

A Review of Remote Sensing Image Fusion Methods

Hassan Ghassemian[*]

Faculty of Electrical and Computer Engineering, Tarbiat Modares University, Tehran, Iran

Email: ghassemi@modares.ac.ir

Abstract

The recent years have been marked by continuous improvements of remote sensors with applications like monitoring and management of the environment, precision agriculture, security and defense. On the one hand, the high spectral resolution is necessary for an accurate class discrimination of land covers. On the other hand, the high spatial resolution is required for an accurate description of the texture and shapes. Practically, each kind of imaging sensor can only focus on a given different operating range and environmental conditions, the reception of all the necessary information for detecting an object or classifying a scene is not possible. So, for the full exploitation of multisource data, advanced analytical or numerical image fusion techniques have been developed. In this paper, we review some popular and state-of-the-art fusion methods in different levels especially at pixel level. In addition to reviewing of different fusion methods, varied approaches and metrics for assessment of fused product are also presented.

Keywords: remote sensing; image fusion; survey; high resolution image.

[*] Corresponding author

1. Introduction

The aim of remote sensing is extraction of information about the Earth's surface structure and content, by acquisition and interpretation of spectral measurements made at a distant location. The spectral, spatial, and temporal variation of electromagnetic energy coming from the scene contains our desired information. In order to produce a high accurate map, the classification process assigns each pixel of the image to a particular class of interest. In remote sensing systems pixels are observed in different portions of electromagnetic spectrum, therefore the remotely sensed images are vary in spectral, spatial and temporal resolution. To collect more photons and maintain image Signal to Noise Ratio (SNR), the multispectral (MS) sensors (with high spectral resolution and narrow spectral bandwidth) have a larger Instantaneous Field Of View (IFOV) (i.e. larger pixel size and lower spatial resolution) compared to panchromatic (PAN) with a wide spectral bandwidth and smaller IFOV (higher spatial resolution) sensors. With appropriate algorithms it is possible to combine these data and produce imagery with the best characteristics of both, namely high spatial and high spectral resolution. This process is known as a kind of multisensor data fusion and also called pansharpening. The fused images may provide increased interpretation capabilities and more reliable results. Performing pansharpening with hyperspectral image is more complex than performing it with MS image. It is expected, because PAN and MS images are acquired almost in the same spectral range while the spectral range of a hyperspectral image is much wider than the one of the corresponding PAN image. Authors in [1] studied and compared different fusion methods for hyperspectral data. In addition to pansharpening, some other applications of image fusion in remote sensing are represented in [2]. The fused image is a combination of two or more geometrically registered images of the same scene into a single image that is more easily interpreted than any of the originals. The fused images can provide more interpretation capabilities and reliable results. The fusion techniques are performed at three different processing levels according to the stage at which the data fusion takes place: pixel level, feature level and decision level. In this paper, we review the popular and state-of-the-art fusion methods in different levels especially in the pixel level. Before that, we briefly represent the different types of sensors and demand for fused remote sensing images.

1.1. Remote sensors

A sensor is an acquisition system. Whereas passive sensors operate using an external energy source, such as sun or the Earth's surface black body emission, active sensors employ an artificial source of radiation as a probe. Satellite Pour l'Observation de la Terre (SPOT) and IKONOS are examples of passive sensors. Synthetic aperture radar (SAR) systems, which typically work in the microwave spectral region through an antenna, and light detection and ranging (LiDAR) scanners, which operate by means of a laser in the optical frequency region, are the most important active sensors [3].

The measurement and recording the energy reflected or emitted by the Earth's, call it $E(x, y, \lambda, t)$, is the basic task of remote sensing (RS). Each measurement is associated to a coordinate system and a function $f(x, y)$ represents an image. In general, f depends on the spatial coordinates (x, y) and the wavelength (λ). Data can be acquired not only in the range between two given wavelengths but also in several channels simultaneously as in the case of MS or hyperspectral (HS) imaging sensors. Moreover, f will depend on time (t) whenever multitemporal observations are considered. f is the representative of an energy that is dependent on the independent variables $\{x, y, \lambda, t\}$. To have the record data in a digital format, spatial coordinates (x, y) are sampled to discrete values based on sampling theory and f is also quantized to discrete values based on quantization theory [4]. In addition, wavelength (λ) will be discretized:

$$f(x, y, \lambda, \mathrm{t}) = \int_{\Delta y} \int_{\Delta x} \int_{\Delta \lambda} \int_{\Delta t} E_r(x, y, \lambda, t) dy dx d\lambda dt \tag{1}$$

As a result, image data is made up of pixels, or discrete picture elements, which each one is characterized by a vector (see Fig. 1).

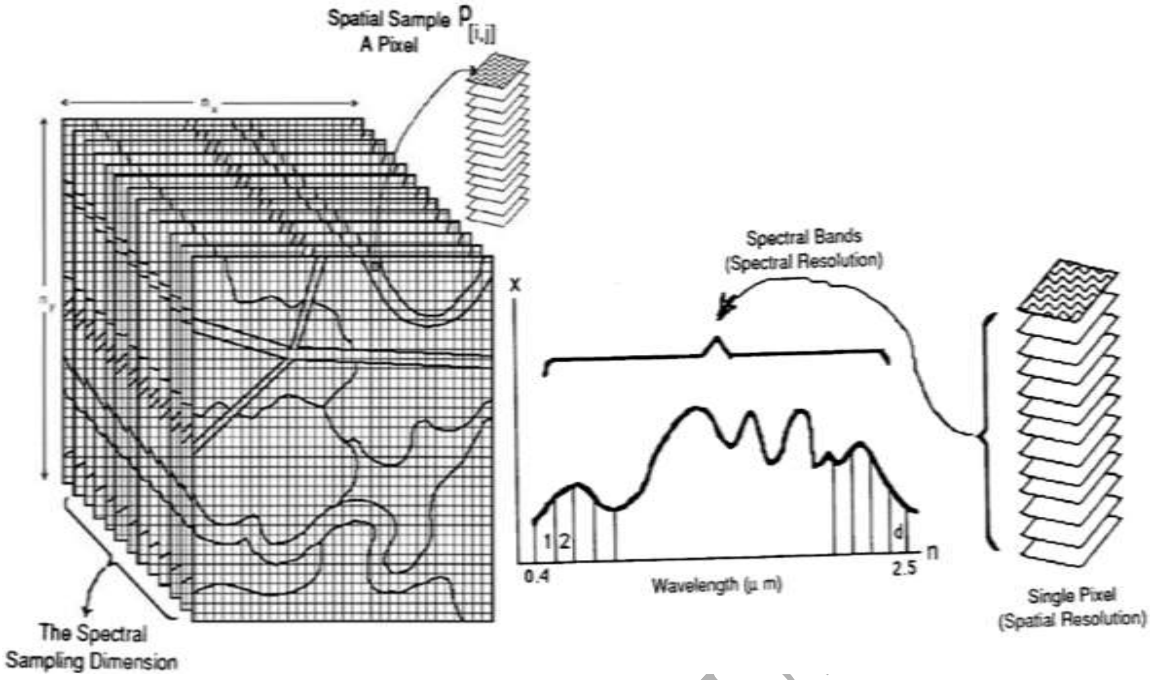

Fig. 1. A typical remote sensing multispectral image data [4].

Temporal resolution or revisit time, the time range between two observations of the same scene, is crucial for the most applications especially in the case of change detection and monitoring. The number of discernible discrete energy values or dynamic range is referred to radiometric resolution. If a sensor has a finer radiometric resolution, it is more sensitive to detect small differences in reflected or emitted energy. Radiometric resolution is usually related to the SNR of a sensor: the better the SNR results higher dynamic range. From the user point of view, the main parameters of a RS acquisition system are spectral, spatial, and radiometric resolutions. The ability to distinguish between point targets, which is dependent on the geometrical properties of the imaging system, is spatial resolution. The capability of a sensor in responding to a specific wavelength interval is spectral resolution. Sensors, depending on their spectral resolution, can be classified as panchromatic, multispectral, superspectral, hyperspectral, and ultraspectral.

A panchromatic sensor operates in a unique broadband. A sensor that integrates the radiation in the visible and near-infrared (V-NIR) spectral range is the most classic example. Thus, the wavelength range is several hundredths of nanometers. The poor spectral resolution of a PAN sensor is usually compensated by its high spatial resolution, that is, of the order of decimeters. A MS sensor operates in several wavelength ranges. Typical MS sensors exhibit three spectral bands in the visible range. Wavelength ranges of MS sensors are narrower than the PAN sensors and one could expect to have wavelength ranges of the order of 50 nm. Due to system constraints, MS sensors operate with a spatial resolution which is lower than PAN sensors. The term superspectral is sometimes used when the number of bands exceeds 10. When the spectral resolution becomes better than 10 nm, the sensors are denoted as HS. An HS sensor can exhibit hundreds of spectral bands. The imaging sensors with spectral resolutions up to the order of 1 nm or less are denoted as ultraspectral. The fusion of MS and HS images is discussed in [5, 6].

1.2. Demand for the fused RS products

The desired information about the Earth's surface structure and content is contained in the spectral, spatial, and temporal variation of electromagnetic energy coming from the scene. The high spectral resolution MS sensors have a lower spatial resolution compared to PAN ones which have a higher spatial resolution and a wide spectral bandwidth. With appropriate combination of these data, we can produce an image with the best characteristics of both, namely high spatial and high spectral resolution. This process is known as a kind of multi-sensor data fusion and called pansharpening of MS image. The fused images may improve the interpretation capabilities and provide more reliable results. Multi-sensor image fusion techniques combine two or more geometrically registered images of the same scene into a single image that is more easily interpreted than any of the originals [7]. PAN and MS images can be obtained by several commercial optical satellites such as SPOT, QuickBird, IKONOS, Landsat, WorldView, GeoEye, OrbView, IRS, Leica ADS40, and Pléiades. In response to why the most satellites do not collect high resolution MS images directly, to meet high spatial and high spectral resolutions, there are two major technical limitations involved: the incoming radiation energy to the sensor, and the data volume collected by the sensor. The size of a PAN detector can be smaller than that of a MS detector to receive the same amount of incoming energy. Therefore, the resolution of the PAN sensor is higher than that of the MS sensor. In addition, a high resolution MS image has a data volume significantly greater than that of a bundled high resolution PAN image and low resolution MS image. Considering these limitations, it is clear that development of an efficient image fusion technique is the best solution for providing high spatial resolution and high spectral resolution remote sensing images. An ideal fusion process should preserves the original spectral characteristics and add spatial characteristics to the image [8].

Image fusion is performed at three different processing levels: 1) pixel level 2) feature level 3) decision level [9] (see Fig. 2). More details about these levels are explained in the next sections.

In addition to fusion of spatial and spectral information, other types of information (such as temporal variation) of remote sensing images can be fused. For example, LANDSAT satellites provide fine resolution images for land cover-mapping [10,11] while the nominal revisit rate of them is only 16 days, and so atmospheric restrictions seriously limit their potential use in monitoring of land cover changes at a seasonal or monthly scale [12]. In contrast, NOAA satellites with moderate resolution imaging spectroradiometer (MODIS) data is acquired twice a day, and therefore, the MODIS instrument is suitable for monitoring dynamic changes of land surfaces [13,14]. Due to physical and financial limitations, no sensor has yet been designed to provide satellite images with both high spatial resolution and high temporal resolution. So, development of models for fusion of the data with a high temporal frequency but coarse spatial resolution with the data that has fine resolution but low temporal frequency is a feasible and less expensive way to obtain this kind of information. A novel regularized spatial and temporal data fusion model based on spatial unmixing has been developed in [15]. The joint use of the high resolution WorldView-2 optical satellite images and the multitemporal TerraSAR-X SAR satellite images to extract the urban buildings height is proposed in [16].

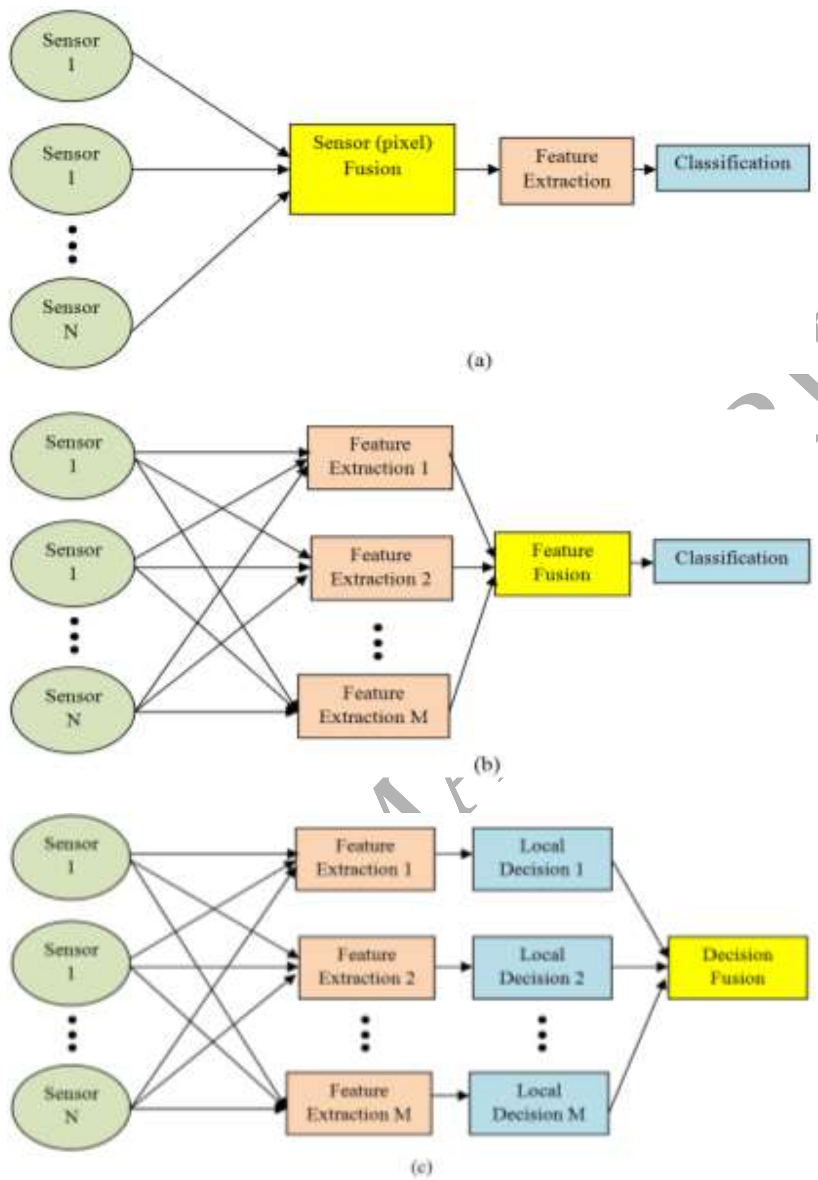

Fig. 2. Fusion levels: a) pixel level, b) feature level, c) decision level.

Authors in [17] summarized the outcome of the 2012 IEEE GRSS multi-modal and multitemporal data fusion contest, including the contributions of three best teams.

Some multi-sensor data fusion methods are discussed in [18]. Even with geometrically registered PAN and MS images, these modalities may have dissimilarities. Some changes may occur in the scene for two different acquisition times. Authors in [19] study relationships between these remotely sensed images for the development of fusion methods. Due to variations between these images, no obvious universal link exists. The main emphasis in [19] is that physics must be taken into account and discuss ways to do so. Because of the complexity of physics and the large number of unknowns, the assumptions are made to drive the development of fusion method. The choice of appropriate assumptions for the development of a method is crucial, with the risk to drastically weaken fusion performance.

The urban remote sensing image data fusion is discussed in [20]. The Data Fusion Committee of the IEEE geoscience and remote sensing society launched a public contest for pansharpening algorithms to identify the ones that perform best in January 2006, testing eight algorithms following different philosophies such as component substitution, multiresolution analysis, detail injection, etc. Several complete data sets from two different sensors, namely, QuickBird and simulated Pléiades were used in this study. The fusion results were collected and evaluated, both visually and objectively in [21] and discussed with more details in [22]. Two algorithms, which basically rely on multi-resolution analysis and employ adaptive models for the injection of high-pass details, have best performance in comparison with the others.

Pohl and van Genderen established a framework for image fusion at the end of the 90s [23], which described and explained mainly pixel based image fusion of Earth observation satellite data, have provided an overview on the advances in image fusion during the past 15 years in [24]. They provided insight into new trends with assembling information about new remote sensing image fusion techniques, recent technical developments and their influence on image fusion, and also introduced the international societies, working groups, and new publications. They presented a categorization of fusion techniques used at pixel level in remote sensing [25].

A survey and discussion on Context-based information fusion is given in [26] providing a comprehensive status of recent and current research on context-based information fusion systems, discussing the current strategies and techniques, and hinting possible future trends. Context-based information fusion processes are done in different levels such as structural and physical constraints of the scenario, a priori known operational rules between entities and environment, dynamic relationships modeled to interpret the system output, and so on. A study of remote sensing image fusion and its application in image classification is done in [27]. In this paper, we review the popular and state-of-the-art fusion methods at the pixel level (section 2), the feature level (section 3), and briefly the decision level (section 4). Moreover, the assessment measures of the fused product are presented in section 5. Finally, section 6 concludes the paper. A brief description of main acronyms used in this paper is reported in Table 1.

Table 1. List of the main acronyms used in this paper.

Acronym	Description
Multispectral	MS
Panchromatic	PAN
Hyperspectral	HS
Component substitution	CS
Multiresolution analysis	MRA
Intensity hue saturation	IHS
Principal component analysis	PCA
Brovey transform	BT
Remote Sensing	RS
Gram-Schmidt	GS

2. Pixel level fusion methods

Multisensor image fusion combines two or more geometrically registered images of the same scene into a single image that is more easily interpreted than any of the originals. The aim is to obtain information of greater quality where the exact definition of greater quality will depend upon the applications [28]. It could mean improvement in further processing [29], better visual appearance [30], or enhancement in visual interpretation of data [31].

The synthesis of MS images at a higher spatial resolution by exploiting a PAN image is usually called pansharpening of MS image. In MS image, the spectral resolution can be up to eight bands, captured in visible and near-infrared wavelength, and the spatial resolution of PAN image can be less than half a meter. We can achieve images with the highest resolutions in the both spectral and spatial domains by fusion of PAN and MS images. The method used for fusion of individual sources must take into account the physical properties of each modality. The fusion algorithms at pixel level are generally divided into four classes: component substitution (CS), multiresolution analysis (MRA), hybrid methods (a combination of CS and MRA), and model based algorithms. Table 2 represents an overview of these classes which will be explained in the following sections.

Table 2. Different classes of fusion methods at pixel level.

Different families of fusion	**Method**	**References**
Component substitution (CS)	IHS and different versions of it	[39],[42],[43]
	Fast IHS	[44],[45],[46]
	Generalized IHS	[47],[48],[49]
	Brovey transform (BT)	[40]
	PCA	[49],[50],[51]
	Gram-Schmidt (GS)	[41]
Multiresolution analysis (MRA)	Decimated wavelet transform	[54], [55]
	Discrete “wavelet packet”	[70]
	Undecimated wavelet transform	[58]
	À trous	[57],[59]
	Laplacian Pyramid	[60]
	Contourlet	[61],[62]
	Multicontourlet	[69]
	Curvelet	[63],[64]
	Curvelet and contourlet	[67]
	Ripplet	[65],[66]
	Multiresolution fusion based on superresolution	[73]
	High-Pass Filter Additive (HPFA)	[71]
	Filter-based	[72]
	Least-squares support vector machine (LS-SVM)	[76]
Hybrid	àtrous wavelet and PCA	[80]
	Combination of wavelet with HIS transform or PCA transform	[79]
	Non-separable wavelet frame transform (NWFT)	[81]
	Wavelet transform and sparse representation	[82]
	Ripplet transform and the compressed sensing	[66]
	ICA and Curvelet	[63]
	ICA and wavelet decomposition	[77]
	Curvelet and IHS	[78]
Model based	Online coupled dictionary learning (OCDL)	[86]
	Spatial correlation modeling	[93]
	MRF model	[89],[90],[91]
	Statistical model	[92],[85],[88]
	Compressive sensing-based (CS) technique	[87]
	Sparse matrix factorization	[6],[88]
	A fast method based on solving a Sylvester equation	[84]
	A hierarchical Bayesian model	[89]

Fusion process must satisfy three conditions [32]: preservation of all relevant information, elimination of irrelevant information and noise, and minimization of artefacts and inconsistencies in the fused image. The noise produced by image sensors can significantly reduce the image fusion quality. Authors in [33] proposed a method for multispectral image fusion and de-noising in the gradient domain. The changes of local details of images can be reflected by the gradients.

Before fusing the images, an image registration algorithm is usually needed to be applied in order to align the source images [34]. In other words, all images to be processed must be coregistered and georeferenced. Low spatial resolution MS images should be resampled into new images with the same resolution as PAN images. The registration errors ignored in the fusion process can significantly affect the fusion quality. A comparison of methods for the geometric and radiometric correction of remote sensing data can be found in [35]. The resampling of the MS image, is usually performed by the means of symmetric digital filtering kernels with odd lengths, that utilize piecewise local polynomials, using linear or cubic interpolation functions. The commercial MS and PAN products are relatively shifted by an odd number of half pixels because their scale ratio is an even number. To compensate the half-pixel shifts between the MS and PAN sampling grids, filters of even lengths may be exploited.

In [36], it is shown that separable polynomial interpolations of odd degrees are feasible with linear-phase kernels of even lengths. As a result, to align the expanded MS with the PAN image, the bi-cubic interpolation, which has the best trade-off between performances and computational complexity, can be applied to commercial MS plus PAN datasets, with no need of performing a further half-pixel registration after interpolation. Some methods such as [37, 38] jointly consider the registration and fusion processes. Since the sensors acquiring the PAN and MS both mounted on the same platforms, pansharpening usually does not require the challenging phase of spatial coregistration with respect to general problem of multisensor fusion.

2.1.CS methods

The CS based methods are based on the projection of MS image into another space using a transformation that separates the spatial structure from the spectral information in different components. Then, the component containing the spatial structure is replaced with the PAN image. The greater correlation between the replaced component and the PAN image, produces less distortion. Thus, we must perform histogram matching between the PAN image and the selected component before its substation. The histogram-matched PAN will have the same mean and variance of the replaced component. Finally, by bringing the data back to the original space through the inverse transformation, the pansharpening process is completed. Intensity-Hue-Saturation (IHS) [39], principal component analysis (PCA) [9], Brovey transform (BT) [40], and Gram-Schmidt (GS) [41] belong to this class of pansharpening.

The IHS transform has high ability to separate the spectral information of an RGB (Red-Green-Blue) composition in its two components, H and S, while isolating most of the spatial information in the I component [42]. A combination of discrete fractional random transform and IHS is proposed in [43]. A fast IHS fusion method is proposed in [44]. In addition to its fast computing capability for fusing images, this method can extend traditional three-order transformations to an arbitrary order. However, the fast IHS fusion as the IHS fusion technique distorts spectrum in the same way. To overcome this problem, authors in [45] consider the minimization problem for a fast IHS method. But, this method is not efficient enough to quickly fuse the high volumes of data from satellite images. Author in [46] provides a fast and easy implementation using a tradeoff parameter. The generalized IHS and HIS-like are introduced in [47] and [48] respectively for fusion of MS images with more than three bands.

PCA is a statistical technique that transforms multivariate data with correlated variables into uncorrelated variables [49]. The first principal component image, PC1, contains the information that is highly correlated to all MS bands used as input to PCA, while the spectral information unique to any of the bands is mapped into other components. Then, PC1 is replaced by the PAN image, which is first stretched to have the same mean and variance as PC1. Authors in [50] applied the PCA transform to the spatial information of the neighboring pixels. Also, they proposed a new hybrid algorithm combining the spectral PCA and spatial PCA methods. In addition to second-order statistics component transforms, data variance-based PCA and SNR-based maximum noise fraction (MNF) transform [51], there are high-order statistics-based components analysis transforms with criteria such as a third-order statistics-based skewness, a fourth-order statistics-based kurtosis, and statistical independence-based independent component analysis (ICA) that requires infinite order of statistics.

The BT transform normalizes the multispectral bands used for a RGB display, and multiplies the result by any other desired data to add the intensity or brightness component to the image.

The GS orthogonalization procedure, which is a powerful pansharpening method, is a generalization of PCA [41]. At first, the MS bands are interpolated at the scale of PAN, and all images are converted to vectors whose dimensions is the number of image pixels at the scale of PAN. Then, the mean of each band is subtracted from all components of the same vector. The synthetic low resolution approximation of the PAN image is used as the first vector of the new orthogonal basis in the orthogonalization procedure. At the time, MS vector is proceeded by finding its projection on the hyperplane defined by the previously found orthogonal vectors and its orthogonal component where the sum of the orthogonal and projection components is equal to the zero-mean version of the original band.

IHS, PCA, BT, and GS techniques are usually characterized by a high fidelity in rendering the spatial details in the fused product, and also they are fast and easy to implement. But, there are some difficulties too. They are limited to cases where the high resolution image (PAN) and the low resolution one (MS) are highly correlated. They are not able to take into account the local differences between MS and PAN images originated by the spectral mismatch between the MS and PAN channels of instruments. So, a significant spectral distortion may be produced. For example, in IHS method, because the histogram-matched PAN and the intensity component do not generally have the same local mean, a large spectral distortion may be noticed as color changes when the fusion result is displayed in color composition. This effect occurs because the spectral response of the intensity channel, synthesized by MS bands, may be far different from that of PAN image. A viable solution is to include the response of the NIR band into the intensity component of MS. However, methods based on injecting zero-mean high-pass spatial details extracted from the PAN have been extensively studied to definitely overcome the inconvenience of spectral distortion.

In addition to direct scheme of CS, i.e., transformation, substitution, and then inverse transformation, there is another formalization which is proposed and analyzed in [52] and [53]. In this formalization of CS, without the explicit calculation of the forward and backward transformations, the fusion process is obtained by using a proper injection scheme. The adaptive CS by partial replacement (PRACS) is introduced in [52], uses the concept of partial replacement of the intensity component, does not use the PAN image directly and defines a new approach to calculate gain. Notice: in the CS approaches, interpolation must guarantee the overlap of MS and PAN at the finer scale.

2.2 MRA methods

In recent years, multi-scale decomposition (MD) based approaches have been successfully applied to image fusion for different applications such as hyperspectral image fusion [54]. Varied MD methods such as pyramid transform and discrete wavelet transform have been applied to image fusion. Three steps can be considered in the MD-based image fusion approaches. At first, the source images are decomposed into several scale levels using a pyramid transform or a wavelet transform. Second, fusion is applied at each level of the source images, and third, the transform is inverted to synthesize the fused image. While the use of the transform increases the computational complexity, the MD-based image fusion approach provides both spatial and frequency domain localization and achieves much better performance. So one can choose or not to employ transforms on images depending on different applications. In the MD-based fusion approaches, the basic fusion rule is applied to the MD representations of images at each resolution level while in the non-MD-based fusion approaches the basic fusion rule is directly applied to the source images. A quantitative comparison, in both spectral and spatial features, to evaluate the wavelet transform and other traditional algorithms is done in [55] and [56]. A wavelet *à trous* ("with holes") algorithm has been proposed in [57].

In the MRA methods, interpolation is less crucial than for the CS methods, because the subsequent step in MRA may realign the details extracted from PAN provided that linear non-zero phase filters are used [36]. As reported in [53], both the MRA and CS methods can be modeled by an injection scheme.

Most multiresolution analysis-based methods employ the wavelet transform, the curvelet transform and the contourlet transform. Famous modalities of MRA that extract the spatial details are: decimated wavelet transform [55], undecimated wavelet transform [58], à trous wavelet transform [59], Laplacian Pyramid [60], contourlet [61, 62], curvelet [63, 64]. In pyramid representation, spatial resolution and image size decrease from one level to the next, while in the wavelet *à trous* algorithm (the spatial resolution decreases from one level to the next) but image size is constant for all levels.

Objects with 1-D singularities can be represented with the wavelet transform. A tensor product of two 1-D wavelet transforms, which resolve 1-D horizontal and vertical singularities, is used for 2-D objects. In the wavelet domain, the fused bands may suffer from a limited number of directional edges and textures. Curvelet and contourlet can resolve 2-D singularities along smooth curves by using a parabolic scaling law. However, they may not sparsely represent any anisotropic structure. Therefore, the ripplet transform is proposed [65]. Two parameters: support c and degree d, which can represent singularities along arbitrarily shaped curves, are introduced in the ripplets. The ripplet transform can be used as an efficient tool for extracting the spatial information from the high spatial/low-spectral PAN images.

Authors in [66] proposed a remote sensing image fusion method based on the ripplet transform and the compressed sensing theory to minimize the spectral distortion in the pansharpened MS bands with respect to the original ones. They extracted the spatial details from the PAN image by means of ripplets and then injected them into MS bands by the proposed injection model named compressed sensing-based injection.

The various multi-resolution decomposition algorithms such as curvelet and contourlet are compared in [67] and the effects of decomposition levels and filters on fusion performance are investigated. The experiments show some results such as: 1-the shift-invariant property has great importance in image fusion, 2-short filter usually provides better fusion results than long filter, and 3-the appropriate setting for the number of decomposition levels is four.

An approach for multiresolution fusion using contourlet transform is proposed in [68]. In this method, the low spatial resolution and high spectral resolution MS image is modeled as the degraded and noisy version of its high spatial resolution version. At first, the initial estimate of the fused image from the available MS image and the PAN image is obtained by the contourlet transform domain learning. The regularization is required to solve this ill-posed problem. For doing regularization, the texture of the final fused image is modeled as a homogeneous Markov random field (MRF), which uses the spatial dependencies among the pixels.

A multicontourlet transform is suitable for representing remote sensing images bearing abundant detailed and directional information with better direction selectivity and energy convergence compared to that of a multiwavelet. An adaptive remote sensing image fusion method based on multicontourlet transform is proposed in [69]. The fusion weight of the low-pass coefficients is selected adaptively based on the golden section algorithm. The local energy feature is employed to select the better coefficients to fusion for the high-frequency directional coefficients.

An image fusion algorithm based on discrete "wavelet packet" transform to fuse multi-sensor images is presented in [70]. When images are fused in the wavelet packet space, different frequency ranges are processed differently. It can fuse information from source images adequately and improve the abilities of information analysis and feature extraction.

High-pass filter additive (HPFA) inserts structural and textural details of the higher resolution image into the lower resolution image. Authors in [71] refined and improved the HPFA fusion method towards a tunable and versatile, yet standardized image fusion tool. Workable sets of HPFA parameters have been derived with regard to high-pass filter properties and injection weights using various input image pairs. The standardization of the HPFA parameters over a wide range of image resolution ratios and the controlled trade-off between sharpness and spectral properties of resulting image are the improvements of this approach.

Authors in [72] designed an optimal filter that is able to extract relevant and non-redundant information from the PAN image. Compared with other kernels such as wavelets, the optimal filter coefficients extracted from statistical properties of images are more consistent with type and texture of remotely sensed images.

The problem of multiresolution fusion is addressed in [73] from a different perspective, based on superresolution techniques. The production of a high spatial resolution image from several low-resolution images, by increasing the maximum spatial frequency and removing the degradations that arise during image acquisition from a low-resolution camera, is the main idea of superresolution. To capture multiple low-resolution observations of the same scene by subpixel shift in the camera motion is the most obvious superresolution method. However, this method requires an accurate registration process, which is a very challenging task. In recent years, image processing researchers have started to exploit learning based methods for image superresolution to overcome this difficulty [74-75]. The advantage of learning-based approaches is that they provide a very natural way to obtain the required image characteristics. The quality of the obtained results can be improved by choosing a proper feature set from training images.

A MS pansharpening method using the multiscale mapped least-squares support vector machine (LS-SVM) is presented in [76]. Under the LS-SVM approach, the salient features underlying the image are represented by support values, and the support value transform is developed for image information extraction. After resampling of the low resolution MS bands to the fine scale of the PAN image, the MS image is sharpened by injecting the detailed features extracted from the high resolution PAN image. Using a series of multiscale support value filters, which are deduced from the mapped LS-SVM with multiscale Gaussian radial basis function kernels, the support value analysis is implemented.

2.3.Hybrid methods

Hybrid methods use the advantages of both the CS and MRA methods with combination of them. An improved ICA fusion method, which uses a wavelet decomposition to extract the detail information of PAN, is proposed in [77]. An image fusion method based on curvelet and ICA is proposed in [63].

A remote sensing image fusion using combining IHS and curvelet transform is proposed and compared with IHS, decimated wavelet transform, wavelet à trous algorithm, ridgelet and curvelet transform in [78].

Different wavelet-based pansharpening methods are available in [79]. In these wavelet-based fusion methods, the high frequency detail coefficients are obtained from the high spatial resolution PAN image and are combined with the spectral information obtained from the MS image through a combination model.

PCA transformation can acquire higher spatial resolution but provides more serious distortion of spectral characteristics. On the other hand, the àtrous wavelet transformation is able to preserve the spatial information while the result has a lack of high spatial resolution. A technique, based on additive wavelet decomposition and PCA transformation is developed for fusing in [80].

A color transfer based fusion algorithm by using the non-separable wavelet frame transform (NWFT) is proposed in [81]. From the source MS image, three bands are selected as the channels to be fused. A grayscale image is generated by averaging these three bands. To obtain a new PAN image with a uniform histogram, as the grayscale image acquired from the source MS image, histogram matching is performed on the source PAN image. The histogram matched PAN image is decomposed using NWFT. In order to produce the composite NWFT coefficients, the lowest frequency subband of the NWFT coefficients is substituted by the grayscale image acquired from the source MS image. A composite image is obtained by performing the inverse NWFT transform on the combined coefficients. Then, three bands selected from the source MS image are mapped into the RGB color space. The color information is transferred into the composite image by using a color transfer method in order to get the final fused image.

A fusion framework that combines the superiorities of wavelet transform and sparse representation is proposed in [82]. In this method, at first, IHS transform is used to separate intensity component from MS image. Then, the filter-based intensity modulation and the wavelet transform are applied to the intensity component of MS and PAN respectively to build the multiscale representations which include the low and high frequency sub-images in different scales. The low and high frequency sub-images are processed with different strategies. While the sparse representation is introduced to the low-frequency sub-images fusion to extract the local structures, the high-frequency sub-images take an image information fusion measurement indicator as the fusion rule. Finally, the inverse wavelet transform and the inverse IHS transform are applied to perform the fusion tasks.

A comparison between nine fusion techniques consist of IHS, Modified IHS, PCA, Wavelet, Local Mean Matching, Local Mean and Variance Matching, Brovey, and Multiplicative fusion techniques are studied on QuickBird data in [83]. The suitability of these approaches for various applications depends on the spectral and spatial quality of the fused images.

2.4 Model based methods

A fast multi-band image fusion is proposed in [84], which forms the likelihoods of the observations. In this fast algorithm, maximizing the likelihoods leads to solving a Sylvester equation. A closed form solution for the Sylvester equation is obtained by exploiting the properties of the circulant and downsampling matrices associated with the fusion problem. This method can be generalized to incorporate prior information for the fusion problem, allowing a Bayesian estimator.

A hierarchical Bayesian model to fuse multiple multi-band images with various spectral and spatial resolutions is proposed in [85]. An appropriate prior distribution is introduced by exploiting geometrical considerations and the posterior distribution is sampled thanks to Hamiltonian Monte Carlo algorithm.

An online coupled dictionary learning (OCDL) approach for image fusion has been introduced in [86]. The OCDL makes the full use of the available lower spatial resolution MS image and the high spatial resolution PAN image to decrease the spectral distortion and preserves the spatial information of the MS image. A superposition strategy is adopted in the OCDL method to produce two intermediate images for the coupled dictionary construction for each band. An iterative update method is utilized to update the coupled dictionaries, which can be referred to as an online dictionary learning process.

The compressive sensing-based fusion technique can greatly reduce the processing time and guarantee the quality of the fused image using fewer non-zero coefficients. However, directly fusing sensing measurements may bring greater uncertain results with high reconstruction error. Moreover, using single fusion rule may result in the problems of blocking artifacts and poor fidelity. In [87], a novel image fusion approach based on compressive sensing is introduced to solve these problems. In this fusion framework, in the first step, the multi-scale transform is performed on each of the pre-registered source images to obtain their low-pass and high-pass coefficients. In the second step, the low-pass bands are merged with a sparse representation based fusion method while the high-pass bands are fused using the absolute values of coefficients as activity level measurement. Finally, the fused image is obtained by performing the inverse multi-scale transform on the merged coefficients. This method is superior to the individual multi-scale transform or sparse representation based methods.

A method for fusing of HS and MS image based on a sparse representation has been introduced in [6]. Authors in [88] used the sparse matrix factorization to present a spatial and spectral fusion model. The proposed method has two stages. In the first stage, the model learns from the low spatial resolution data a spectral dictionary containing pure signatures, and in the second stage, the desired high spatial resolution and high spectral resolution data are predicted using the learned spectral dictionary and the known high spatial resolution data.

Generally, the main drawback of the pixel-level fusion rule is that the decision on whether a source image contributes to the fused image is made pixel by pixel and, this may cause spatial distortion in the merged image. In a source image, if one of its pixels contributes to the fused image, its neighbors are also likely to contribute to the fused image because the pixels in an image are spatially correlated. Therefore, the decision making during the first step of the fusion process should exploit the property of spatial correlation to improve fusion performance. The use of a window- or region-based method is a straightforward approach to make use of spatial correlation. The MRF theory provides a basis for modeling contextual constraints in visual processing and interpretation [89]. An MRF model has been used to model the images for the fusion of edge information [90]. In [91], two fusion algorithms by incorporating the contextual constraints via MRF models into the fusion model have been proposed. The first algorithm models the decision making at the first step of the fusion rule as an MRF, and is applicable for both the MD-based fusion approach and the non-MD-based fusion approach. The second algorithm models both the decision making and the true image as MRFs and is only applicable for the non-MD-based fusion approach. A statistical model to describe the fusion process is proposed in [92].

3. Feature level fusion methods

Feature level fusion methods deal with data at higher processing levels than pixel level methods. Normally, at first, feature extraction procedures are applied. Then, the fusion process using advanced techniques takes place. For example, the extraction of objects using segmentation procedures is required in fusion at feature level. Features correspond to characteristics, which are depending on their environment such as shape, extent and neighborhood, are extracted from the original images. The similar objects from multiple sources are assigned to each other and then fused for further assessment. Table 3 shows several fusion methods at feature level which are represented with more details in the following. Authors in [93] used a combination of texture and shape features extracted from HS images, as well as spectral information, in order to increase the classification accuracy.

Table 3. Different fusion methods at feature level.

Method	References
A combination of texture, shape, and spectral information	[93]
Integrating hierarchical segmentation results into MRF	[89]
Multirate filter banks	[94],[95]
Retina based multi-resolution	[96]
Learning-based superresolution fusion	[100]
Softmax regression-based feature fusion	[101]

A new spectral-spatial classification method for HS images, which is based on integrating hierarchical segmentation results into Markov random field spatial prior in the Bayesian framework, is proposed in [89].

The multirate filter banks are proposed in [94]. Let the low-resolution (Δ_1) sensor produces an N_1 by N_1image, called $f_L(x,y)$, and the high-resolution (Δ_2) sensor generates an N_2 by N_2 image, called $f_H(x,y)$. The Fourier transform of the low resolution and high resolution images, as a feature extraction process of images, in the spatial-frequency domain are given by $F_L(u,v)$ and $F_H(u,v)$, respectively and calculated as follows:

$$F_L(u,v) = \sum_{x=1}^{N_1} \sum_{y=1}^{N_1} f_L(x\Delta_1 + y\Delta_1)\, e^{-j2\pi(xu+yv)\Delta_1} \tag{2}$$

$$F_H(u,v) = \sum_{x=1}^{N_2} \sum_{y=1}^{N_2} f_H(x\Delta_2 + y\Delta_2)\, e^{-j2\pi(xu+yv)\Delta_2} \tag{3}$$

It is obvious that, the low-resolution image is located in the low-frequency region, and the high-resolution image occupies the higher frequency and this suggests a multi-resolution scene representation. In other words, this scheme is based on multirate filter banks image synthesizer: the energy packing the spectral features are distributed in the lower frequency subbands, and the spatial features, edges, are distributed in the higher frequency subbands [95]. Let $H(u,v)$ be a low spatial resolution filter of N_1, and $G(u,v)$ is the high spatial resolution filter of N_2. In the spatial-frequency domain, feature level data fusion can synthesis a MS high resolution image of the scene with the spatial resolution of N_2, $F_{H_{fused}}(u,v)$, as follows (see Fig. 3):

$$\boldsymbol{F_{H_{fused}}(u,v) = H(u,v)F_L(u,v) + G(u,v)F_H(u,v)} \quad (4)$$

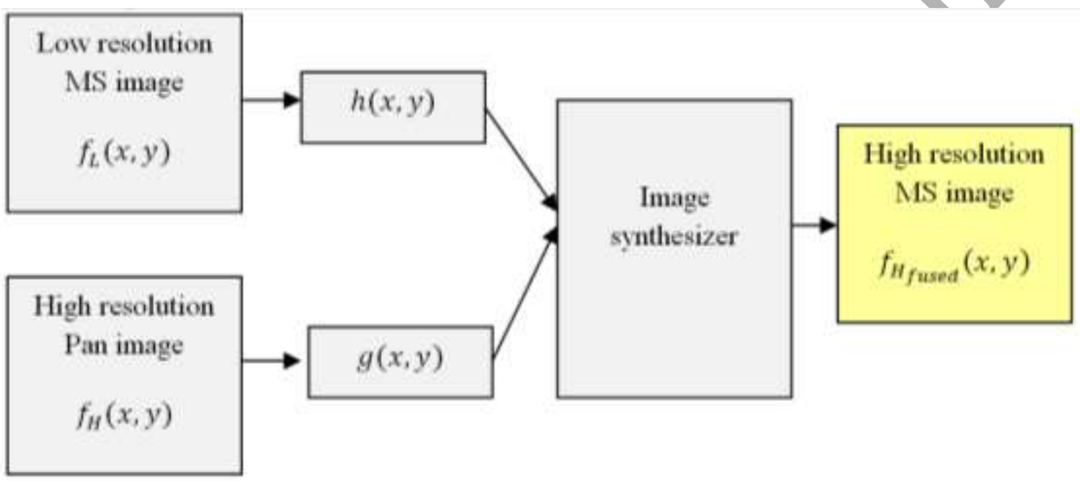

Fig. 3. The proposed multi-resolution image fusion procedure in [94].

In this fusion method, there is no need to resample images, which is an advantage over IHS, PCA, Brovey and wavelet methods. It can perform in any aspect ratio between the PAN image and MS images' pixels.

The biological retina is really more than a simple imagery camera. It not only converts the optical information into the electrical signals but also performs considerable processing on the visual signal before transmitting it to higher visual system levels. Based on this knowledge, image fusion can incorporate the processing principles of human vision system. A multi-resolution data fusion scheme, based on retinal visual channels decomposition is proposed in [96] (see Fig. 4).

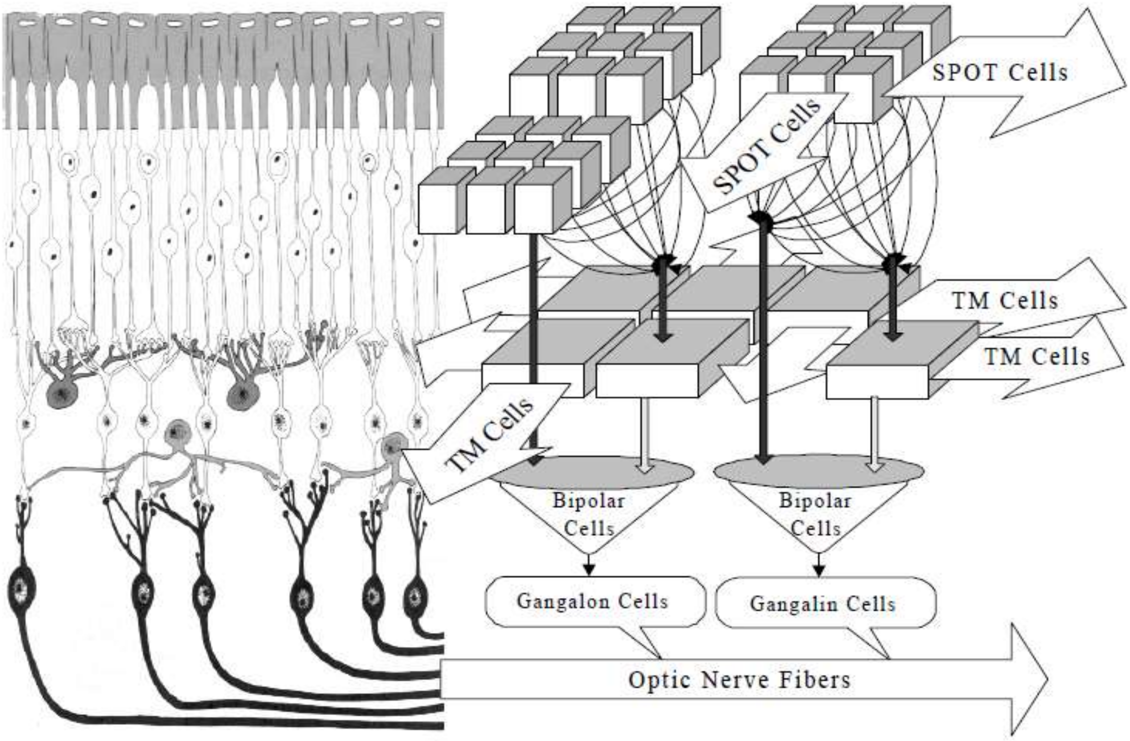

Fig. 4. The Retina based multi-resolution image fusion proposed in [96].

It is motivated by analytical results obtained from retina based image analysis: the energy packing the spectral features are distributed in the lower frequency subbands and the spatial features are distributed in the higher frequency subbands. The high-scale spatial features, extracted from the PAN image, are added to the low-scale spatial features from thematic mapper (TM) images. As a result, the visual-channels procedure enhances the MS images. The computer retina inspired model presented in [96] is based on difference-of-Gaussian (DOG) operator, which describes some of the receptive field properties of the ganglion cells:

$$\boldsymbol{DOG(r,\sigma_s) = \alpha_c G(r;\sigma_c) - \alpha_s G(r;\sigma_s)} \tag{5}$$

where $\boldsymbol{\alpha_c}$ and $\boldsymbol{\alpha_s}$ are weights of center and surround inputs. Both $\boldsymbol{G(r;\sigma_c)}$ and $\boldsymbol{G(r;\sigma_s)}$ are spatially lowpass filters where $\boldsymbol{r = \sqrt{x^2 + y^2}}$ is the two-dimensional spatial position and

$$\boldsymbol{G(r;\sigma) = \frac{1}{2\pi\sigma^2} exp\,\frac{-|r|^2}{2\sigma^2}} \tag{6}$$

The retinal based model consists of five layers (see Fig. 4). The first layer represents an array of high resolution receptors and the second layer is the high-scale spatial feature extractor. The function of this layer is represented by the following operator:

$$\boldsymbol{h_1}(\boldsymbol{r}) = \frac{\Delta_1^2}{2\pi}\, \boldsymbol{exp}\{-|\boldsymbol{r}\Delta_1|^2\} - \frac{\Delta_2^2}{2\pi}\, \boldsymbol{exp}\{-|\boldsymbol{r}\Delta_2|^2\} \quad (7)$$

where Δ_1 and Δ_2 are the high-resolution pixel size and the low-resolution pixel size respectively. The array of low resolution receptors (horizontal cells) composes the third layer. This layer's function is modeled by:

$$\boldsymbol{h_2}(\boldsymbol{r}) = \frac{\Delta_2^2}{2\pi}\, \boldsymbol{exp}\{-|\boldsymbol{r}\Delta_2|^2\} \quad (8)$$

The fourth and the fifth layers consist of bipolar and ganglion cells. The function of these layers can represented by:

$$f(x,y) = h_1(x,y) \otimes f_1(x,y) + h_2\,(x,y) \otimes f_2\,(x,y) \quad (9)$$

where $f_1(x,y)$and $f_2\,(x,y)$ are the high and low resolution images respectively. This allows to generate a spatially enhancing MS image, $f(x,y)$, by adding the high-resolution spatial features to $f_2\,(x,y)$.

In the retina based fusion method, there is no need to resample images, which is an advantage over IHS, PCA, Brovey and wavelet methods. It can perform in any aspect ratio between the PAN image and MS images' pixels. It is important to avoid the resampling process as much as possible because it degrades the spectral features of the MS images in any image merging method.

In addition to remote sensing, the retina-based model is used to fuse magnetic resonance imaging (MRI) and positron emission tomography (PET) images [97,98] in medical applications. The PET exhibits good functional characteristic and MRI has high spatial resolution. The PET image indicates the brain function and has a low spatial resolution while the MRI image shows the brain tissue anatomy and contains no functional information. Hence, the image fusion is used to enhance the spatial resolution of the functional image by combining it with a high-resolution anatomic image. A combination of feature and pixel level image fusion with feedback retina and IHS model is proposed in [99]. A learning-based superresolution fusion method is proposed in [100], which combines the swath width and spectral properties of Landsat TM/Enhanced TM Plus (ETM+) and the spatial resolution of SPOT5.

To do object classification, various types of features can be extracted from very high resolution remote sensing images. The classification performance can benefit from proper feature fusion. Authors in [101] have proposed a softmax regression-based feature fusion method by learning distinct weights for different features. In this method, object-to-class similarity measures and the conditional probabilities that each object belongs to different classes are estimated. Moreover, an approximate method for calculating the class-to-class similarities between different classes is introduced. Finally, a support vector machine classifier is build using the obtained fusion and similarity information.

4. Decision level fusion methods

Decision fusion (or interpretation level) is the highest processing level. It is the process of merging information from several individual data sources after each data source has undergone a preliminary classification. In the decision level fusion, the received results from different local classifiers will be combined to determine the final decision. In other words, the input images are processed individually for information extraction. Then, the decision rules are used to combine extracted information to reinforce common interpretation and resolve differences and furnish a better understanding of the observed objects. The input decisions are some labels or symbols with different degrees of confidence. Table 4 shows several fusion methods at decision level which are represented with more details in the following.

Table 4. Different fusion methods at decision level.

Method	References
Hybrid methods based on consensus	[103]
Voting	[104]
Rank-based	[106]
Bayesian inference	[110]
Dempster-Shafer	[105]
Joint Measures Method	[107]
Fuzzy decision rule	[108]
Adaptive decision fusion based on the local scale of the structure	[109]

Decision level fusion has great uses in the distributed and parallel processing systems. Fusion methods are applied in varied applications such as remote sensing image classification, fingerprint verification. Decision-level fusion of different verification methods is a challenge for improvement of fingerprint verification especially when the quality of images is low. In [102], the idea of decision level fusion of orientation, texture, and spectral features of fingerprint image is represented.

Hybrid classification methods based on consensus from several data sources are considered in [103]. The concentration is on the statistical and neural network methods and the combination of those approaches. At first, each data source is treated separately and modeled using statistical methods. After that, weighting mechanisms are used to control the influence of each data source in the combined classification. In order to improve the combined classification accuracies, the weights are optimized.

Some of useful decision fusion methods, applied in different applications, are voting [104], rank-based, Bayesian inference and Dempster-Shafer methods [105-106].

There is a main problem in the voting methods: they suffice to local classification results for local winner class in its defined pixel, which causes an intensive decrease in accuracies of decision fusion results for the obtained class-correlated data. The rank-based method has more attention on data than voting methods. It uses the results of local classification for a defined pixel, but in all classes. In this method, the results of local classification should include the classification measure values (or rank) of all classes, which causes intensive increases in the data volume of local classifiers outputs, the input of decision fusion center, and communication systems between local classifier and fusion center.

The Bayesian method does not consider uncertainty and may have error and complexity in the posterior probabilities measurements. When the number of unknown propositions is larger than the number of known propositions, the probabilities calculated by the Bayesian method can become unstable. The Dempster-Shafer method, which is an extension of the Bayesian inference, can be used without prior probability distributions and so is able to deal with uncertainty and overcomes some of the drawbacks.

The authors in [107] introduced the joint measures method as a powerful method for the development of a high performance multi-sensor image fusion scheme at the decision level. The images are received from distributed multiple sensors, in different spectral bands such as visible, infrared, thermal and microwave. They extract the mathematical properties of multi-sensor local classification results and use them for modeling of the classifier performances by the two measures: the plausibility and correctness. Then, they establish the plausibility and correctness distribution vectors and matrices for introducing two improvements of the Dempster-Shafer method. After that, they introduce the joint measures decision fusion method based on using these two measures jointly. The joint measures method, can deal with any decision fusion problem in the case of uncertain local classifiers results as well as clear local classifiers results.

A method for fusion of multiple classifiers, which provides redundant or complementary results, is proposed in [108]. In the first step, data is processed by each classifier separately, and for each pixel, membership degrees for the considered classes are provided. In the second step, the results provided by the algorithms according to the classifiers' capabilities are aggregated using a fuzzy decision rule. A general framework, based on the definition of two measures of accuracy, for combining information from several individual classifiers in multiclass classification is proposed. The first measure is a pointwise measure which estimates, for each pixel, the reliability of the information provided by each classifier. The second measure estimates the global accuracy of each classifier. The results are aggregated with an adaptive fuzzy operator ruled by these two measures.

The assessment of the quantitative quality of the pansharpened images shows that *à trous* wavelet transform-based pansharpening and Laplacian pyramid-based context adaptive pansharpening methods outperform each other depending upon the local content of the scene. Therefore, the proposed method in [109] takes the advantage of both methods by locally selecting the best one. In other words, this adaptive decision fusion is performed based on the local scale of the structure.

In [110], decision level fusion in multiviews imagery is used in an object recognition strategy. The proposed method contains two stages: single view and multiviews. In the first stage, the object-based image analysis is performed independently on the individual views. In the second stage, in order to refine the classification results, the classified objects of all views are fused together through a decision level fusion based on the scene contextual information.

5. Assessment of fused product

Many image fusion techniques have been proposed to fuse the PAN and MS images effectively. However, it is important to assess the quality of the fused image in various applications of remote sensing. The main limitation for the evaluation of fused product is the absence of the reference image. There are some main approaches to cope with this problem. The first approach uses the quality indexes that needs no reference image, but operates on the relationships among the original and pansharpened images. This approach directly operates on data at native scale, but, the definition of indexes biases the obtained results. The second approach considers the images at a spatial resolution lower than the original and considers the original MS image as a reference (Wald's protocol). In the third approach, that needs no reference image, the approximations of MS and PAN images are obtained from the fused images. Then, the approximated MS is compared with the original MS and the approximated PAN is compared with the original PAN.

5.1. Quality measures

Many researchers have proposed different quality metrics in terms of both qualitative and quantitative analyses. The performance of the fused image by visual comparison between the fused image and raw input images is determined by qualitative analysis. On the other hand, the performance of the fused image is determined by quantitative analysis using two main approaches: with reference image and without reference image.

A review of metrics available in the literature, for assessing the quality of fused image, is presented in [111]. Some of assessment measures of fused product, which divided into two groups, are represented in the following.

5-1-1- Measures which require the reference image such as:

- Spectral angle mapper (SAM) [112], which calculates the angle between the corresponding pixels of the fused and the reference image.
- The root mean square error (RMSE), which is the root mean square difference between the reference and the fused image.
- The Erreur Relative Globale Adimensionnelle de Synthèse (ERGAS) [113], which is composed by a sum of RMSE values.
- The universal image quality index or Q-index [114], which comprises an estimate of correlation coefficient and the differences in the mean luminance and in the contrast.
- Q4 vector index [115], which is a vector extension of the Q-index and used for datasets composed by four spectral bands.
- $Q2^n$-index [116], which is a generalization of Q4-index for images with a number of spectral bands greater than four.

Some other metrics are mean bias, percentage fit error, SNR, peak signal to noise ratio, correlation coefficient, mutual information, and structural similarity index measure.

An efficient tool to assess the geometrical performance in fusion, through the analysis of the quality of selected contours, is the modulation transfer function (MTF) [117]. The MTF is the modulus of the Fourier transform of the point spread function (PSF) [118] which is an important characteristic of optical instruments. MTF describes the image quality in terms of contrast as a function of spatial frequency. The MTF of MS and PAN images are different from each other due to their different sampling rates. This difference must take into account when the fused image is synthesized at the PAN spatial resolution. The MTF of fused image can be estimated and compared with that of reference image to quantify the geometrical quality of the synthesized image.

5-1-2- Measures which do not require the reference image such as:

- Quality with no reference (QNR) index [119], which quantifies the spectral and spatial distortions, composed by the product, weighted by some coefficients, of two separate values.
- Standard deviation
- Entropy and cross entropy
- Spatial frequency
- Fusion mutual information
- Fusion quality index
- Fusion similarity metric.

Generally a high spatial resolution MS image as reference is required in the assessment indices, which is not always readily available. Moreover, the fusion quality assessments using these indices may not be consistent with the human visual system (HVS). To overcome this inconsistency, an HVS-consistent image fusion quality assessment index without a reference MS image is proposed in [120]. The spatial details and spectral information of original and fused images are first separated in Gaussian scale space, and the qualities are evaluated using the proposed spatial and spectral quality index respectively.

By a combination of the proposed two indices, the overall quality is determined without a reference MS image.

5.2.Wald's protocol

Pyramid representation with a multi-resolution analysis using a multi-scale model is the basis of most ARSIS implementations [121]. In Fig. 5, the pyramid representation is shown. In this figure, A_0 and B_1 are the original PAN and MS images respectively. A_1, A_2, A_3, … are the successive coarser approximations of the PAN image, and B_2, B_3, B_4, … are the successive coarser approximations of the MS image. B^*_0 is the fused image.

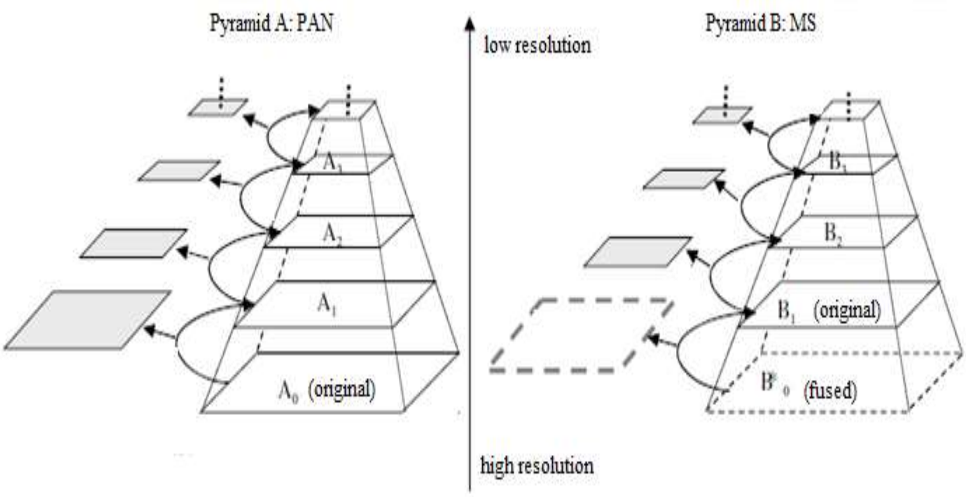

Fig. 5. The pyramid representation in MRA approach [121].

The protocols introduced in [122] comprise the checking of two properties: the consistency property and the synthesis property. According to consistency property, the fused image (B^*_0) should be equal to the original image (B_1) after being downsampled to its original low resolution $(B^*_0)_1$. According to the synthesis property, original images are downsampled to reach lower resolution (A_0 is resampled to A_1 and B_1 is resampled to B_2). These two new images are fused to produce an image at original low resolution of the MS image. So, the original MS set is obviously considered as reference image. The quality of fused image assessed at this low resolution is assumed to be close to the one found at the highest resolution.

The protocols of [122] use the hypothesis “the quality assessment drawn at low resolution is assumed close to or worse than the one that which would have been drawn at high resolution if the reference images are available”. This hypothesis is often verified in practice but not always. In [123], some results are found: 1- this hypothesis is not validated when the images are noisy. 2- The verification of the hypothesis strongly depends upon the quality budget and the ratio. 3- The quality of the fusion process has certainly an impact on the relationship of this hypothesis.

5.3. Second protocol

The second protocol for assessment of fused product is shown in Fig. 6. At first, PAN and MS images are fused to produce the fused image F.

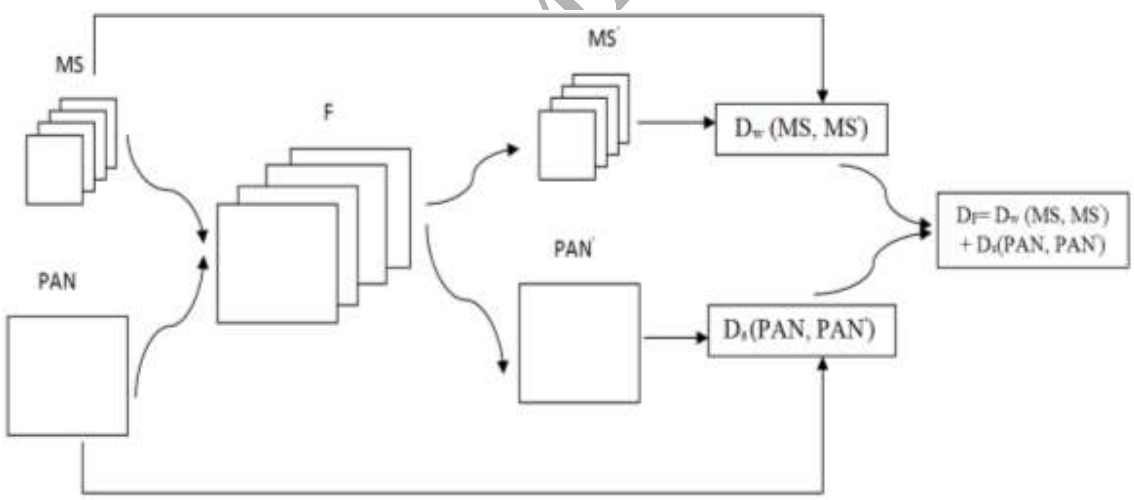

Fig. 6. The Second protocol.

To assess the quality of F, there are the following steps:

1- We downsample F to produce the low resolution version of it at the scale of original MS. The result is called $MS^{'}$. Then, we calculate the dissimilarity between MS and $MS^{'}$, i.e., D_w (MS,

$MS^{'}$). The used dissimilarity measure can be any distance measure that can calculates the spectral differences between two multispectral images, for example SAM.

2- We obtain an approximation of the PAN image ($PAN^{'}$) from the F image using the weighted summation of spectral bands of F as represented in (2). Then, we calculate the dissimilarity between PAN and $PAN^{'}$, i.e., D_s (PAN, $PAN^{'}$). The used dissimilarity measure can be any distance measure that can calculates the spatial differences between two single PAN images, for example ERGAS.

3- Finally, the summation of spectral and spatial dissimilarities obtained in previous steps is used to assess the quality of fused image, i.e., $D_F = D_w$ (MS, $MS^{'}$) + D_s (PAN, $PAN^{'}$). The smaller the value D_F, the better quality the fused image will have.

4- Because human vision is less sensitive to spectral distortions, but it is very sensitive to spatial variation, we can show the amount of SAM(x,y) or ERGAS(x,y) or D_F(x,y) in spatial domain as an image (see Fig. 7 [87]).

$$SAM(x,y) = \arccos\left(\frac{\left\langle f(x,y), \hat{f}(x,y)\right\rangle}{\left\| f(x,y)\right\| \left\| \hat{f}(x,y)\right\|}\right) \quad (10)$$

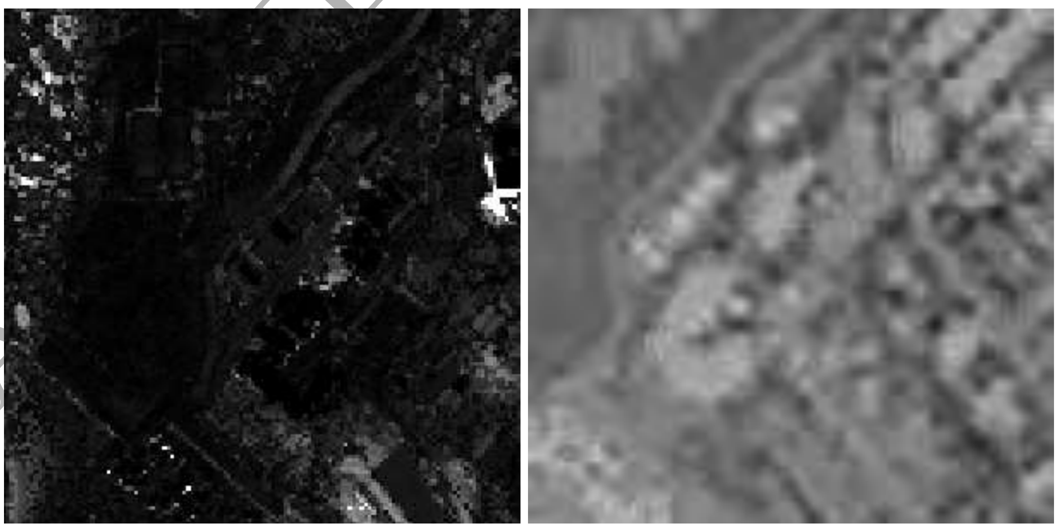

Fig. 7. Spectral angle mapper each pixel SAM(x,y), which calculates the angle between the corresponding pixels of the fused and the reference image in the left and the ERGAS(x,y) on the right.

The traditional quality assessment methods focus on the spectral information at the data level but fail to indicate the image content at the information level, which is more important for specific remote sensing applications. The first results of MS and PAN images fusion for the ZY-3 satellite, which is China's first civilian high-resolution satellite, have been announced in [124]. A set of information indices that are able to describe the image content for the fusion quality assessment are used to investigate the performance of commonly used pansharpening techniques. Four primitive information indices are employed: the morphological building/shadow indices and the normalized vegetation/water indices. These indices can be automatically calculated without the need for machine learning or training samples. Therefore, they can directly reflect the image content.

6. Conclusion

Information fusion is a hot research topic in remote sensing image processing. The specific objectives of image fusion are as follows: to improve the spatial resolution, to improve the classification accuracy, to enhance the capabilities of features display, to improve the geometric precision, to enhance the capability of the change detection and to replace or repair the defect of image data. We focused on the pixel level remote sensing image fusion in this paper. The reviewed methods are located in four different classes: CS, MRA, hybrid, and model based approaches. CS methods are generally fast and easy to implement. But, they may produce significant spectral distortions. In contrast to CS methods, MRA methods cause a higher spatial distortion but a superior spectral consistency. To take the advantage of both methods, hybrid methods were introduced. To have an intuitive interpretation of the fusion process, the fusion of MS and PAN images can be conveniently formulated within a model such as the Bayesian inference framework. The assessment of fused product can be done with or without need to a reference image with different approaches which each one has its advantages and disadvantages. The former approach needs to a rescaling of images and the later approach is done at native scale.

References

[1] L. Loncan, L. B. Almeida, J. M. Bioucas-Dias, X. Briottet, J. Chanussot, N. Dobigeon, S. Fabre, W. Liao, G. Licciardi, M. Simoes, J-Y. Tourneret, M. Veganzones, G. Vivone, Q. Wei and N. Yokoya, Hyperspectral pansharpening: a review, IEEE Geoscience and remote sensing magazine, 3 (3) (2015) 27-46.

[2] E. Basaeed, H. Bhaskar, M. Al-Mualla, Beyond Pan-sharpening: Pixel-level Fusion in Remote Sensing Applications, in: proceedings of the International Conference on Innovations in Information Technology, 2012, pp. 139 – 144.

[3] L. Alparone, B. Aiazzi, S. Baronti, A. Garzelli, Remote Sensing Image Fusion, CRC Press, Taylor & Francis Group, New York, 2015.

[4] Hassan Ghassemian and David Landgrebe, On-Line Object Feature Extraction for Multispectral Scene Representation, NASA NAGW-925, TR-EE 88-34, Aug.1988.

[5] F. Palsson, J. R. Sveinsson, M. Orn Ulfarsson, J.Atli Benediktsson, Model Based Fusion of Multi- and Hyperspectral Images Using PCA and Wavelets, IEEE Transactions on Geoscience and Remote Sensing, 53 (5) (2015) 2652 - 2663.

[6] Q. Wei, J. Bioucas-Dias, N. Dobigeon, J.-Y. Tourneret, Hyperspectral and Multispectral Image Fusion Based on a Sparse Representation, IEEE Transactions on Geoscience and Remote Sensing, 53 (7) (2015) 3658 - 3668.

[7] Y. Zhang, Understanding Image Fusion, Photogrammetric Engineering & Remote Sensing (2004) 657-661.

[8] H. Ghassemian, Multi-sensor image fusion by inverse subband coding, International Archives of Photogrammetry and Remote Sensing, Vol. XXXIII, Supplement B2. Amsterdam 2000, pp. 20-27.

[9] C. Pohl, Multisensor image fusion in remote sensing, review article, International Journal of Remote Sensing, 19 (5) (1998) 823-854.

[10] J. Knorn , A. Rabe, V. C. Radeloff, T. Kuemmerle, J. Kozak, P. Hostert, Land cover mapping of large areas using chain classification of neighboring Landsat satellite images, Remote Sensing of Environment, 11 (5) (2009) 957–964.

[11] J.G. Masek, E.F. Vermote, N.E. Saleous, R. Wolfe, F.G. Hall, K.F. Huemmrich, F. Gao , J. Kutler, T.-K. Lim, A Landsat surface reflectance dataset for North America, 1990–2000, IEEE Geoscience and Remote Sensing Letters, 3 (1) (2006) 68–72.

[12] M. C. Gonzalez-Sanpedro, T. Le-Toan, J. Moreno, L. Kergoat, E. Rubio, Seasonal variations of leaf area index of agricultural fields retrieved from Landsat data, Remote Sensing of Environment, 112 (3) (2008) 810–824.

[13] N. C. Strugnell, W. Lucht, C. Schaaf, A global albedo data set derived from AVHRR data for use in climate simulations, Geophysics Research Letters, 28 (1) (2001) 191–194.

[14] J. J. Walker, K. M. de Beurs, R. H. Wynne, F. Gao, Evaluation of Landsat and MODIS data fusion products for analysis of dryland forest phenology, Remote Sens. Environ., 175 (2012) 381–293.

[15] Y.Xu, B. Huang, Y. Xu, K. Cao, C. Guo, D. Meng, Spatial and Temporal Image Fusion via Regularized Spatial Unmixing, IEEE Geoscience and Remote Sensing Letters, 12 (6) (2015) 1362-1366.

[16] Y. Xu, P. Ma, E. Ng, H. Lin, Fusion of WorldView-2 Stereo and Multitemporal TerraSAR-X Images for Building Height Extraction in Urban Areas, IEEE Geoscience and Remote Sensing Letters,12 (8) (2015) 1795-1799.

[17] C. Berger, M.Voltersen, R. Eckardt, J. Eberle, T. Heyer, N. Salepci, S. Hese, C. Schmullius, J. Tao, S. Auer, R. Bamler, K. Ewald, M. Gartley, J. Jacobson, A. Buswell, Q. Du, F. Pacifici, Multi Modal and Multi-Temporal Data Fusion: Outcome of the 2012 GRSS Data Fusion Contest, IEEE Journal of Selected Topics in Applied Earth Observations and Remote Sensing, 6 (3) (2013) 1324-1340.

[18] G. Simone, A. Farina, F.C. Morabito, S.B. Serpico, L. Bruzzone, Image fusion techniques for remote sensing applications, Information Fusion, 3 (2002) 3–15.

[19] C. Thomas, T. Ranchin, L. Wald, J. Chanussot, Synthesis of Multispectral Images to High Spatial Resolution: A Critical Review of Fusion Methods Based on Remote Sensing Physics, IEEE Transactions on Geoscience and Remote Sensing, 46 (5) (2008) 1301-1312.

[20] P. Gamba, F. Dell_Acqua, B. V. Dasarathy, Urban remote sensing using multiple data sets: Past, present, and future, Information Fusion, 6 (2005) 319–326.

[21] A. Garzelli, F. Nencini, Fusion of panchromatic and multispectral images by genetic algorithms, in: proceedings of the IEEE International Geoscience and Remote Sensing Symposium, 2006, pp. 3810–3813.

[22] L. Alparone, L. Wald, J. Chanussot, C. Thomas, P. Gamba, L. Mann Bruce, Comparison of Pansharpening Algorithms: Outcome of the 2006 GRS-S Data-Fusion Contest, IEEE Transactions on Geoscience and Remote Sensing, 45 (10) (2007) 3012-3021.

[23] C. Pohl, J. L. Van Genderen, Review article, Multisensor image fusion in remote sensing: concepts, methods and applications, International Journal of Remote Sensing, 19 (5) (1998) 823-854.

[24] C. Pohl, J. L. Van Genderen, Remote sensing image fusion: an update in the context of Digital Earth, International Journal of Digital Earth, 7 (2) (2014) 158–172.

[25] C. Pohl, J. L. Van Genderen, Review Article, Structuring contemporary remote sensing image fusion, International Journal of Image and Data Fusion, 6 (1) (2015) 3–21.

[26] L. Snidaro, J. Garcia, J. Llinas, Context-based Information Fusion: A survey and discussion, Information Fusion, 25 (2015) 16–31.

[27] W. Wenbo,Y. Jing,K. Tingjun, Study of Remote Sensing Image Fusion and Its Application In Image Classification, The International Archives of the Photogrammetry, Remote Sensing and Spatial Information Sciences, 2008, pp. 1141-1146.

[28] L. Wald, Some terms of reference in data fusion, IEEE Transactions on Geoscience and Remote Sensing, 37 (3) (1999) 1190–1193.

[29] G. Piella, A general framework for multiresolution image fusion: from pixels to regions, Information Fusion, 4 (4) (2003) 259-280.

[30] Y. Zhang, Understanding image fusion, Photogrammetric engineering and remote sensing, 70 (6) (2004) 657-661.

[31] J. J. Lewis, R. J. O'Callaghan, S. G. Nikolov, D. R. Bull, C. N. Canagarajah, Region-based image fusion using complex wavelets, The 7th International Conference on Information Fusion, 2004, pp. 555–562.

[32] O. Rockinger, Pixel level fusion of image sequences using wavelet frames, in: proceedings of the 16th Leeds Annual Statistical Research Workshop, 1996, pp. 149–154.

[33] W. Zhao, Z. Xu, J. Zhao, Gradient entropy metric and p-Laplace diffusion constraint-based algorithm for noisy multispectral image fusion, Information Fusion, 27 (2016) 138–149.

[34] P. K. Varshney, B. Kumar, M. Xu, A. Drozd, I. Kasperovich, Image registration: A tutorial, in: proceedings of the IEEE NATO advance Science institutes series, 2005.

[35] P. Cheng, T. Toutin, C. Pohl, A comparison of geometric models for multisource data fusion. Remote Sensing, GIS and GPS in Sustainable Development and Environmental Monitoring, GeoInformatics '95, in: proceedings of the International Symposium, 1995, pp. 11- 17.

[36] B. Aiazzi, S. Baronti, M. Selva, L. Alparone, Bi-cubic interpolation for shift-free pan-sharpening, ISPRS Journal of Photogrammetry and Remote Sensing, 86 (2013) 65–76.

[37] Q. Zhang, Z. Cao, Z. Hu, Y. Jia, X. Wu, Joint Image Registration and Fusion for Panchromatic and Multispectral Images, IEEE Geoscience and Remote Sensing Letters, 12 (3) (2015) 467-471.

[38] Y. Li, Z. He, H. Zhu, W. Zhang, Y. Wu, Jointly registering and fusing images from multiple sensors, Information Fusion, 27 (2016) 85–94.

[39] W. Carper, T. Lillesand, R. Kiefer, The use of intensity-huesaturation transformations for merging SPOT panchromatic and multispectral image data, Photogrammetric Engineering and Remote Sensing, 56(4) (1990) 459-467.

[40] Earth Resource Mapping Pty Ltd, The Brovey transform explained, EMU Forum, 2 (11) (1990), available in http: // www. ermapper.com/ forum_new/emuf2-11.htm # aiticle_5.

[41] C. A. Laben, B. V. Brower, Process for enhancing the spatial resolution of multispectral imagery using pan-sharpening, U.S. Patent 6011875 A (2000).

[42] H. Chu, W. Zhu, Fusion of IKONOS Satellite Imagery Using IHS Transform and Local Variation, IEEE Geoscience and Remote Sensing Letters, 5 (4) (2008) 653-657.

[43] Q. Guo, A. Li, H. Q. Zhang, Z. K. Feng, Remote Sensing Image Fusion Based on Discrete Fractional Random Transform for Modified HIS, International Archives of the Photogrammetry, Remote Sensing and Spatial Information Sciences, 2013, pp. 19-22.

[44] T.-M. Tu, P. S. Huang, C.-L. Hung, C.-P. Chang, A fast intensity-hue-saturation fusion technique with spectral adjustment for IKONOS imagery, IEEE Geoscience and Remote Sensing Letters, 1 (4) (2004) 309–312.

[45] M. González-Audícana, J. L. Saleta, R. G. Catalán, R. García, Fusion of multispectral and panchromatic images using improved IHS and PCA mergers based on wavelet decomposition, IEEE Transactions on Geoscience and Remote Sensing, 42 (6) (2004) 1291–1299.

[46] M. Choi, A New Intensity-Hue-Saturation Fusion Approach to Image Fusion With a Tradeoff Parameter, IEEE Transactions on Geoscience and Remote Sensing, 44 (6) (2006) 1672-1682.

[47] X. Zhou, J. Liu, S. Liu, L. Cao, Q. Zhou, H. Huang, A GIHS-based spectral preservation fusion method for remote sensing images using edge restored spectral modulation, ISPRS Journal of Photogrammetry and Remote Sensing, 88 (2014) 16–27.

[48] T.-M. Tu, S.-C. Su, H.-C. Shyu, P. S. Huang, A new look at IHS-like image fusion methods, Information Fusion, 2 (3) (2001) 177–186.

[49] M. González-Audícana, J. L. Saleta, R. G. Catalán, R. García, Fusion of multispectral and panchromatic images using improved IHS and PCA mergers based on wavelet decomposition, IEEE Transactions on Geoscience and Remote Sensing, 42 (6) (2004) 1291–1299.

[50] H. R. Shahdoosti, H. Ghassemian, Combining the spectral PCA and spatial PCA fusion methods by an optimal filter, Information Fusion, 27 (2016) 150–160.

[51] A. A. Green, M. Berman, P. Switzer, M. D. Craig, A transformation for ordering multispectral data in terms of image quality with implications for noise removal, IEEE Transactions on Geoscience and Remote Sensing, 26 (1988) 65–74.

[52] J. Choi, K. Yu, Y. Kim, A new adaptive component-substitution based satellite image fusion by using partial replacement, IEEE Transactions on Geoscience and Remote Sensing, 49 (1) (2011) 295–309.

[53] G. Vivone, L. Alparone, J. Chanussot, M. Dalla Mura, A. Garzelli, G. A. Licciardi, R. Restaino, L. Wald, A Critical Comparison Among Pansharpening Algorithms, IEEE Transactions on Geoscience and Remote Sensing, 53 (5) (2015) 2565 – 2586.

[54] Y. Zhang, S. De Backer, P. Scheunders, Noise-resistant waveletbased Bayesian fusion of multispectral and hyperspectral images, IEEE Transactions on Geoscience and Remote Sensing, 47 (11) (2009) 3834–3843.

[55] J. Zhou, D. Civo, J. Silander, A wavelet transform method to merge Landsat TM and SPOT panchromatic data, Int. J. Remote Sensing, 19 (4) (1998) 743-757.

[56] J. Nunez, X. Otazu, O. Fors, A. Prades, V. Pala, R. Arbiol, Multiresolution based image fusion with additive wavelets decomposition, IEEE Transactions on Geoscience and Remote Sensing, 37 (3) (1999) 1204-1211.

[57] M.V. Joshi, L. Bruzzone, S. Chaudhuri, A model-based approach to multiresolution fusion in remotely sensed images, IEEE Transactions on Geoscience and Remote Sensing, 44 (9) (2006) 2549-2562.

[58] G. P. Nason, B. W. Silverman, The stationary wavelet transform and some statistical applications, in wavelets and Statistics, A. Antoniadis and G. Oppenheim, Eds. New York, NY, USA: Springer- Verlag, 103 (1995) 281–299.

[59] M. J. Shensa, The discrete wavelet transform: Wedding the à trous and Mallat algorithm, IEEE Transactions on Signal Processing, 40 (10) (1992) 2464–2482.

[60] P. J. Burt, E. H. Adelson, The Laplacian pyramid as a compact image code, IEEE Transactions on Communications, COM-31 (4) (1983) 532–540.

[61] M. N. Do, M. Vetterli, The contourlet transform: An efficient directional multiresolution image representation, IEEE Transactions on Image Processing, 14 (12) (2005) 2091–2106.

[62] V. P. Shah, N. H. Younan, R. L. King, An efficient pan-sharpening method via a combined adaptive PCA approach and contourlets, IEEE Transactions on Geoscience and Remote Sensing, 46 (5) (2008) 1323–1335.

[63] M. Ghahremani, H. Ghassemian, Remote-sensing image fusion based on Curvelets and ICA, International Journal of Remote Sensing, 36 (16) (2015) 4131–4143.

[64] M. Choi, R. Y. Kim, M. R. Nam, H. O. Kim, Fusion of multispectral and panchromatic satellite images using the curvelet transform, IEEE Geoscience and Remote Sensing Letters, 2 (2) (2005) 136–140.

[65] J. Xu, L. Yang, D. Wu, Ripplet: A new transform for image processing, Journal of Visual Communication and Image Representation, 21 (7) (2010) 627–639.

[66] M. Ghahremani, H. Ghassemian, Remote Sensing Image Fusion Using Ripplet Transform and Compressed Sensing, IEEE Geoscience and Remote Sensing Letters, 12 (3) (2015) 502-506.

[67] S. Li, B. Yang, J. Hu, Performance comparison of different multi-resolution transforms for image fusion, Information Fusion, 12 (2011) 74–84.

[68] K. P. Upla, M. V. Joshi, P. P. Gajjar, An Edge Preserving Multiresolution Fusion: Use of Contourlet Transform and MRF Prior, IEEE Transactions on Geoscience and Remote Sensing, 53 (6) (2015) 3210-3220.

[69] X. Chang, L. Jiao, F. Liu, F. Xin, Multicontourlet-Based Adaptive Fusion of Infrared and Visible Remote Sensing Images, IEEE Geoscience and Remote Sensing Letters, 7 (3) (2010) 549-553.

[70] H.-H. Wang, J.-X. Peng, W. Wu, A Fusion Algorithm of Remote Sensing Image Based on Discrete Wavelet Packet, in: proceedings of the Second International Conference on Machine Learning and Cybernetics, 2003, pp. 2557-2562.

[71] U. G. Gangkofner, P. S. Pradhan, D. W. Holcomb, Optimizing the High Pass Filter Addition Technique for Image Fusion, Photogrammetric Engineering & Remote Sensing, 74 (9) (2008) 1107–1118.

[72] H. R. Shahdoosti, H. Ghassemian, Fusion of MS and PAN Images Preserving Spectral Quality, IEEE Geoscience and Remote Sensing Letters, 12 (3) (2015) 611-615.

[73] M. V. Joshi, L. Bruzzone, S. Chaudhuri, A Model-Based Approach to Multiresolution Fusion in Remotely Sensed Images, IEEE Transactions on Geoscience and Remote Sensing, 44 (9) (2006) 2549-2562.

[74] M. V. Joshi, S. Chaudhuri, P. Rajkiran, A learning based method for image superresolution from zoomed observations, IEEE Transactions on Systems, Man, and Cybernetics, Part B: Cybernetics, 35 (3) (2005) 527–537.

ACCEPTED MANUSCRIPT

[75] M. V. Joshi, S. Chaudhuri, R. Panuganti, Super-resolution imaging: Use of zoom as a cue, Image and Vision Computing, 22 (14) (2004) 1185–1196.

[76] S. Zheng, W.-Z. Shi, J. Liu, J. Tian, Remote Sensing Image Fusion Using Multiscale Mapped LS-SVM, IEEE Transactions on Geoscience and Remote Sensing, 46 (5) (2008) 1313-1322.

[77] F. Chen, F. Qin, G. Peng, S. Chen, Fusion of Remote Sensing Images Using Improved ICA Mergers Based on Wavelet Decomposition, 2012 International Workshop on Information and Electronics Engineering, Procedia Engineering 29 (2012) 2938-2943.

[78] S. A.Valizadeh, H. Ghassemian, Remote Sensing Image Fusion Using Combining HIS and Curvelet Transform, 6'th International Symposium on Telecommunications, 2012, pp. 1184-1189.

[79] J. Nunez, X. Otazu, O.I. Fors, A. Prades, V. Pala, R. Arbiol, Multiresolution-based image fusion with additive wavelet decomposition, IEEE Transactions on Geoscience and Remote Sensing, 37 (3) (1999) 1204-1212.

[80] Y. Luo, R. Liu, Y. Feng Zhu, Fusion of Remote Sensing Image Base on The PCA+ATROUS Wavelet Transform, The International Archives of the Photogrammetry, Remote Sensing and Spatial Information Sciences, Vol. XXXVII (Part B7), 2008, pp. 1155-1158.

[81] Z. Li, Z. Jing, X. Yang, S. Sun, Color transfer based remote sensing image fusion using non-separable wavelet frame transform, Pattern Recognition Letters, 26 (2005) 2006–2014.

[82] J. Cheng, H. Liu, T. Liu, F. Wang, H. Li, Remote sensing image fusion via wavelet transform and sparse representation, ISPRS Journal of Photogrammetry and Remote Sensing, 104 (2015) 158–173.

[83] K. G. Nikolakopoulos, Comparison of Nine Fusion Techniques for Very High Resolution Data, Photogrammetric Engineering & Remote Sensing, 74 (5) (2008) 647–659.

[84] Q. Wei, N. Dobigeon, J.-Y. Tourneret, Fast Fusion of Multi- Band Images Based on Solving a Sylvester Equation, IEEE Transactions on Image Processing, 24 (11) (2015) 4109-4121.

[85] Q. Wei, N. Dobigeon, J.-Y. Tourneret, Bayesian fusion of multi-band images, IEEE Journal of Selected Topics in Signal Processing, 9 (6) (2015) 1117-1127.

[86] M. Guo, H. Zhang, J. Li, L. Zhang, H.Shen, An Online Coupled Dictionary Learning Approach for Remote Sensing Image Fusion, IEEE Journal of Selected Topics in Applied Earth Observations and Remote Sensing, 7 (4) (2014) 1284-1294.

[87] M. Ghahremani, H. Ghassemian, A Compressed-Sensing-Based Pan-Sharpening Method for Spectral Distortion Reduction, IEEE Transactions on Geoscience and Remote Sensing, In Press. (DOI: 10.1109/TGRS.2015.2497309).

[88] B. Huang, H. Song, H. Cui, J. Peng, Z. Xu, Spatial and Spectral Image Fusion Using Sparse Matrix Factorization, IEEE Transactions on Geoscience and Remote Sensing, 52 (3) (2014) 1693-1704.

[89] M. Golipour, H. Ghassemian, F. Mirzapour, Integrating Hierarchical Segmentation Maps With MRF Prior for Classification of Hyperspectral Images in a Bayesian Framework, IEEE Transactions on Geoscience and Remote Sensing, In Press. (DOI: 10.1109/TGRS.2015.2466657)

[90] W. Wright, Fast image fusion with a Markov random field, in: proceedings of the Seventh International Conference on Image Processing and Its Applications, 1999, pp. 557–561.

[91] M. Xu, H. Chen, P. K. Varshney, An Image Fusion Approach Based on Markov Random Fields, IEEE Transactions on Geoscience and Remote Sensing, 49 (12) (2011) 5116-5127.

[92] R. S. Blum, On multisensor image fusion performance limits from an estimation theory perspective, Information Fusion, 7 (3) (2006) 250–263.

[93] F. Mirzapour, H. Ghassemian, Improving hyperspectral image classification by combining spectral, texture, and shape features, International Journal of Remote Sensing, 36 (4) (2015) 1070–1096.

[94] H. Ghassemian, Muilti-Sensor Image Fusion Using Multirate Filter Banks, in: IEEE proceedings of the International Conference on Image Processing, 2001, pp. 846-849.

[95] H. Ghassemian, A.Venetsanopoulos, Image Coding Using Vector Quantization in LP Space, 1998 IEEE Symposium on Advances in Digital Filtering and Signal Processing, 1998, pp. 7-11.

[96] H. Ghassemian, A Retina Based Multi-Resolution Image Fusion, in: proceedings of the IEEE International Geoscience and Remote Sensing Symposium, 2001, 709-711.

[97] S. Daneshvar, H. Ghassemian, MRI and PET image fusion by combining IHS and retina-inspired models, Information Fusion, 11 (2010) 114–123.

[98] S. Daneshvar, H. Ghassemian, MRI and PET images fusion based on human retina model, Journal of Zhejiang University SCIENCE A, 8 (10) (2007) 1624-1632.

[99] S. Daneshvar, H. Pourghassem, M. Danishvar, H. Ghassemian, Combination of Feature and Pixel Level Image Fusion with Feedback Retina and IHS Model, IAENG International Journal of Computer Science, 38 (3) (2011).

[100] H. Song, B. Huang, Q. Liu, K. Zhang, Improving the Spatial Resolution of Landsat TM/ETM+ Through Fusion With SPOT5 Images via Learning Based Super-Resolution, IEEE Transactions on Geoscience and Remote Sensing, 53 (3) (2015) 1195-1204.

[101] X. Bai, C. Liu, P. Ren, J. Zhou, H. Zhao, Y. Su, Object Classification via Feature Fusion Based Marginalized Kernels, IEEE Geoscience and Remote Sensing Letters, 12 (1) (2015) 8-12.

[102] S. Helfroush, H. Ghassemian, Nonminutiae-Based Decision-Level Fusion for Fingerprint Verification, EURASIP Journal on Advances in Signal Processing, (2007) 1-11.

[103] J. Atli Benediktsson, J. R. Sveinsson, P. H. Swain, Hybrid Consensus Theoretic Classification, IEEE Transactions on Geoscience and Remote Sensing, 35 (4) (1997) 833-843.

[104] L. O. Jimenez, A. Morales-Morell, A. Creus, Classification of Hyperdimensional Data Based On Feature and Decision Fusion Approaches Using Projection Pursuit, Majority Voting, and Neural Networks, IEEE Transactions on Geoscience and Remote Sensing, 37 (3) (1999), 1360–1366.

[105] Z. Hongwei, O. Basir, F. Karray, Data fusion for pattern classification via the dempstershafer evidence theory, IEEE International Conference on Systems, Man and Cybernetics, 2002, pp. 109–110.

[106] A. Rashidi, H. Ghassemian, Extended dempster-shafer theory for multi system/sensor decision fusion, Workshop on Challenges in Geospatial Analysis, Integration and Visualization, 2003.

[107] A. J. Rashidi, M. H. Ghassemian, A New Approach for Multi System/Sensor Decision Fusion Based on Joint Measures, International Journal of Information Acquisition, 1 (2) (2004) 109–120.

[108] M. Fauvel, J. Chanussot, J. Atli Benediktsson, Decision Fusion for the Classification of Urban Remote Sensing Images, IEEE Transactions on Geoscience and Remote Sensing, 44 (10) (2006) 2828-2838.

[109] B. Luo, M. Murtaza Khan, T. Bienvenu, J. Chanussot, L. Zhang, Decision Based Fusion for Pansharpening of Remote Sensing Images, IEEE Geoscience and Remote Sensing Letters, 10 (1) (2013) 19-23.

[110] F. Tabib Mahmoudi, F. Samadzadegan, P. Reinartz, Jr., Object Recognition Based on the Context Aware Decision-Level Fusion in Multiviews Imagery, IEEE Journal of Selected Topics in Applied Earth Observations and Remote Sensing, 8 (1) (2015) 12-22.

[111] P. Jagalingam, A. Vittal Hegde, A Review of Quality Metrics for Fused Image, International Conference on Water Resources, Coastal and Ocean Engineering, 2015, pp. 133 – 142.

[112] R. H. Yuhas, A. F. H. Goetz, J. W. Boardman, Discrimination among semi-arid landscape endmembers using the Spectral AngleMapper (SAM) algorithm, in: proceedings of Summaries of the Third Annual JPL Airborne Geoscience Workshop**,** 1992, pp. 147–149.

[113] L. Wald, Quality of high resolution synthesized images: Is there a simple criterion? in: proceedings of the third conference "Fusion of Earth data: merging point measurements, raster maps and remotely sensed images", 2000, pp 99-103.

[114] Z.Wang, A. C. Bovik, A universal image quality index, IEEE Signal Processing Letters, 9 (3) (2002) 81–84.

[115] L. Alparone, S. Baronti, A. Garzelli, F. Nencini, A global quality measurement of pan-sharpened multispectral imagery, IEEE Geoscience and Remote Sensing Letters, 1 (4) (2004) 313–317.

[116] A. Garzelli, F. Nencini, Hypercomplex quality assessment of multi-/ hyper-spectral images, IEEE Geoscience and Remote Sensing Letters, 6 (4) (2009) 662–665.

[117] C.Thomas, L.Wald, A MTF-based distance for the assessment of geometrical quality of fused products, in: IEEE proceedings of Fusion, 2006, pp. 10-13.

[118] P. Massip, Ph. Blanc, L. Wald, Data fusion: taking into account the modulation transfer function in ARSIS based pansharpening methods, in: proceedings of the 29th Symposium of the European Association of Remote Sensing Laboratories, 2009. pp. 424-431.

[119] L. Alparone, B. Aiazzi, S. Baronti, A. Garzelli, F. Nencini, M. Selva, Multispectral and panchromatic data fusion assessment without reference, Photogrammetric Engineering & Remote Sensing, 74 (2) (2008) 193–200.

[120] J. Liu, J. Huang, S. Liu, H. Li, Q. Zhou, J. Liu, Human visual system consistent quality assessment for remote sensing image fusion, ISPRS Journal of Photogrammetry and Remote Sensing, 105 (2015) 79–90.

[121] C.Thomas, J.-C. Laneri, T. Ranchin, L. Wald, A modular platform for fusion of images, in: proceedings of the 4th International Conference on Physics in Signal Image Processing (PSIP), 2005, pp. 269-273.

[122] L. Wald, T. Ranchin, M. Mangolini, Fusion of satellite images of different spatial resolutions: assessing the quality of resulting images, Photogrammetric Engineering & Remote Sensing, 63 (6) (1997) 691-699.

[123] C. Thomas, L. Wald, Analysis of changes in quality assessment with scale, in: IEEE proceedings of Fusion, 2006, pp.147.

[124] X. Huang, D.Wen, J. Xie, L.Zhang, Quality Assessment of Panchromatic and Multispectral Image Fusion for the ZY-3 Satellite: From an Information Extraction Perspective, IEEE Geoscience and Remote Sensing Letters, 11 (4) (2014) 753-757.